

## MICROSTRUCTURE AND NONLINEAR PROPERTIES OF Zn-V-Mn-Nb-O VARISTOR CERAMICS WITH Nd<sub>2</sub>O<sub>3</sub> SUBSTITUTION

N. H. ISA<sup>a</sup>, A. ZAKARIA<sup>a\*</sup>, R.S. AZIS<sup>a,b</sup>, W.R.W. ABDULLAH<sup>c</sup>

<sup>a</sup>*Department of Physics, Faculty of Science, Universiti Putra Malaysia, 43400 UPM Serdang, Selangor, Malaysia*

<sup>b</sup>*Institute of Advanced Materials, Universiti Putra Malaysia, 43400 UPM Serdang, Selangor, Malaysia*

<sup>c</sup>*School of Ocean Engineering, Universiti Malaysia Terengganu, 21030 Kuala Terengganu, Terengganu, Malaysia*

An abnormal grain growth of the ZnO-based ceramics due to highly reactive vanadium liquid phase disrupts its nonlinear properties. The effect of Nd<sub>2</sub>O<sub>3</sub> concentration from 0.01 to 0.05 mol% on microstructure and electrical properties of ZnO-based varistor ceramics were investigated. The sample was fabricated via solid state method and sintered at 900 °C for 2 h. XRD analysis shows the V<sub>2</sub>O<sub>5</sub> and Zn<sub>2</sub>Nb<sub>2</sub>Mn<sub>2</sub>O<sub>9</sub> phase formation. SEM analysis shows the grain is more uniform and enlarged to 3.54 μm with Nd<sub>2</sub>O<sub>3</sub> addition up to 0.03 mol%. Nd<sub>2</sub>O<sub>3</sub> also increased both the nonlinear coefficient  $\alpha$  and the breakdown electric field,  $E_{1mA}$  to an optimum of 9.94 and 75 V/mm. Beyond that concentration, oxygen O vacancy formed at the grain boundary and diminished the electrical properties.

(Received April 23, 2017; Accepted August 16, 2017)

**Keywords:** ZnO, Nd<sub>2</sub>O<sub>3</sub>, low-voltage varistor

### 1. Introduction

Electronic device exhibit an excellent property in low operating voltage but are very susceptible to either transient or permanent overvoltage. The nonlinear electrical properties of varistor divert the current created by the excessive voltage away from the protected electronic device. ZnO-based varistor ceramics made by sintering ZnO powder modified with selected additives such as CoO, Sb<sub>2</sub>O<sub>3</sub>, MnO<sub>2</sub> and Cr<sub>2</sub>O<sub>3</sub> together with Bi<sub>2</sub>O<sub>3</sub> as main additives [1-3]. Its nonlinear properties are ascribed to a double Schottky barrier (DSB) formed at active grain boundaries containing many trap states [4,5].

The ZnO-V<sub>2</sub>O<sub>5</sub>-based varistor ceramics exhibit good nonlinear properties, strongest accelerated degradation characteristics and densified at relatively low temperature in the vicinity of about 900 °C [6-11]. However, the microstructure of ceramics is nonuniform which contribute to high leakage current at about milli-Ampere (mA). In the early development of ZnO-V<sub>2</sub>O<sub>5</sub>-based systems, the sample exhibit an exaggerated grain growth due to highly reactive of V<sub>2</sub>O<sub>5</sub> where its kinetic grain growth exponent is 1.44 smaller than ZnO-Bi<sub>2</sub>O<sub>3</sub>-based and pure ZnO-based systems which are 5 and 3, respectively [7]. Then, MnO<sub>2</sub> and Nb<sub>2</sub>O<sub>5</sub> doped into ZnO-V<sub>2</sub>O<sub>5</sub>-based system show a better improvement in the microstructure where the grain boundary is clearly separated [9-14]. The fast grain growth of the systems is reduced with an addition of 2 mol% MnO<sub>2</sub> where its kinetic grain growth exponent is 4 [6]. The rare earth oxide incorporation into ZnO-based varistor ceramics would control the grain growth from conglomerating into a large grain and improved the nonlinearity of varistors by increasing the surface state density through the formation of interstitial states and deep bulk traps [15-19].

Numerous studies on the effect of rare earth oxide (REO) additives such as Gd<sub>2</sub>O<sub>3</sub>, Dy<sub>2</sub>O<sub>3</sub>, and Er<sub>2</sub>O<sub>3</sub> on the Zn-V-Mn-Nb-O varistor ceramic systems sintered at 900°C for 3 hrs shows that it exhibit good varistor properties in the amount as low as 0.05 mol% [20-22]. Interestingly, Gd<sub>2</sub>O<sub>3</sub>

\*Corresponding author: hasanah5152@yahoo.com

substitution possessed a high breakdown voltage about 5365 V/cm with 1 mm thickness for high voltage application at 0.05 mol% Gd<sub>2</sub>O<sub>3</sub> [22]. Nahm (2011) and Nahm (2015) reported an incorporation of 0.05 mol% Er<sub>2</sub>O<sub>3</sub> and 0.1 mol% Dy<sub>2</sub>O<sub>3</sub> into that systems increased the breakdown voltage to 5444 and 5117 V/cm with similar bulk thickness [20,21]. The high breakdown voltage is an important parameter to determine the practical application of varistor. For commercial low voltage application, the breakdown voltage are in range between 82 V to 120 V with bulk thickness range between 5 to 10 mm. Although the ceramic systems has been studied in many aspect for high voltage application [20-22], the studies of REO substitution effect on the varistor properties of the Zn-V-Mn-Nb-O varistor ceramic systems for low voltage varistor application have not been attempted. So it is necessary to find the specific concentration for low voltage varistor application by focusing on Nd<sub>2</sub>O<sub>3</sub> concentration below 0.05 mol%. It is hypothesized that incorporation of Nd<sub>2</sub>O<sub>3</sub> concentration below 0.05 mol% is expected to improve the microstructure and nonlinear properties of ZnO based varistors for low voltage varistor application. So, it is useful to study the Nd<sub>2</sub>O<sub>3</sub> effect on ZnO-based varistor properties sintered at 900 °C at low concentration. In this paper, the effect of Nd<sub>2</sub>O<sub>3</sub> concentration below 0.05 mol% on microstructure and electrical properties of Zn-V-Mn-Nb-O varistor ceramics were discussed to determine its potential for low voltage varistor application. In this paper, the effect of Nd<sub>2</sub>O<sub>3</sub> incorporation at concentration below 0.05 mol% on the microstructure and electrical properties of ZnO-based ceramics varistors were discussed.

## 2. Experimental

### 2.1. Sample Preparation

The sample was fabricated according to (97.4-x)ZnO(x)Nd<sub>2</sub>O<sub>3</sub>(0.5)V<sub>2</sub>O<sub>5</sub>(2)MnO<sub>2</sub>(0.1)Nb<sub>2</sub>O<sub>5</sub> from high-purity reagent-grade raw materials (> 99.9%, Alfa Aesar) where  $x$  is 0.01, 0.02, 0.03, 0.04 and 0.05 mol%. Raw materials were ground using ball milling with zirconia balls with distilled water for 24 h. The slurry was dried at 70 °C for 12 h before adding the binder polyvinyl alcohols 1.75 wt% and then sieving through the 75 µm mesh screen. The powder from each ceramic combination was pressed into pellets with 10 mm diameter and 1 mm in thickness at a pressure of 4 tonne/m<sup>2</sup>. The pellets were sintered at a temperature of 900 °C in air for 2 h with heating and cooling rates of 5 °C/min.

### 2.2 Microstructure and density measurement

The crystalline phase was identified using Cu K $\alpha$  radiation ( $\lambda = 1.540598 \text{ \AA}$ ) with PANalytical X'Pert. XRD software X'Pert high score software Pro PW3040/60) was used to analyse crystalline phases. The surface microstructure were examined by a scanning electron microscope (SEM, model: LEO 1455 VPSEM). One side of the samples was lapped and ground with SiC paper, and then polished with 0.3 µm Al<sub>2</sub>O<sub>3</sub> powder to make a mirror-like surface. The average grain size ( $D$ ) was determined by the linear intercept method through expression

$$D = \frac{1.56L}{MN} \quad (1)$$

where  $L$  is the length of a random line drawn on a micrograph of sample surfaces,  $M$  is the micrograph magnification,  $N$  is the number of grain boundaries intercepted by the line, and 1.56 is the correction factors required for converting the  $D$  from average intercept diameter [23,24]. The average density ( $\rho_{\text{avg}}$ ) of sintered sample was determined using an electronic densimeter (Alfa Mirage, Model MD-300S), working based on the Archimede's principle. The relative density ( $\rho_{\text{rel}}$ ) was calculated by using expression

$$\rho_{\text{rel}} = \frac{\rho_{\text{avg}}}{\rho_{\text{theoretical}}} \times 100\% \quad (2)$$

where the  $\rho_{\text{theoretical}}$  of ZnO is 5.65 g/cm<sup>3</sup>.

### 2.3 Electrical measurement

The current density  $J$ -electric field  $E$  characteristics at room temperature were measured using a low-voltage source-measure (Keithley Model 2410) unit to obtain pellet sample non-linear coefficient ( $\alpha$ ). The measurement was performed by varying the applied voltage between 0 to 100 V. All samples were coated with silver conductive paint and cured at 550 °C for 10 min to make the electrodes. The nonlinear coefficient  $\alpha$  value was determined from  $J$ - $E$  plot through the expression

$$\alpha = \frac{\log J_2 - \log J_1}{\log E_2 - \log E_1} \quad (3)$$

where  $E_1$  and  $E_2$  are the electric fields corresponding to  $J_1 = 1$  mA/cm<sup>2</sup> and  $J_2 = 10$  mA/cm<sup>2</sup>, respectively. The breakdown field ( $E_{1\text{mA}}$ ) was measured at 1 mA/cm<sup>2</sup> in the current density and the leakage current density ( $J_L$ ) was measured at 0.8  $E_{1\text{mA}}$ . It is well accepted that thermionic emission is the predominant conduction mechanism in the pre-breakdown region. For this reasons, the potential barrier height  $\phi_B$  could be estimated according to

$$J = AT^2 \exp\left(\frac{\beta E^{1/2} - \phi_B}{k_B T}\right) \quad (4)$$

where  $k_B$  is the Boltzmann constant ( $8.167 \times 10^{-5}$  eV/K),  $A$  is the Richardson's constant ( $30$  A/cm<sup>2</sup>K<sup>2</sup>) for ZnO,  $T$  is the absolute temperature,  $\beta$  is a constant related to the relation as  $\beta \sim (r\omega)^{-1}$ , where  $r$  is grains per unit length and  $\omega$  is the barrier width [25].

## 3. Results and Discussion

Fig. 1 shows the XRD patterns of the sample at 0.01, 0.02, 0.03, 0.04 and 0.05 mol% of Nd<sub>2</sub>O<sub>3</sub>. The major diffraction peaks belong to ZnO as primary phase, while the minor diffraction peaks show the existence of V<sub>2</sub>O<sub>5</sub> phase at position 25.53° and Zn<sub>2</sub>Mn<sub>2</sub>Nb<sub>2</sub>O<sub>9</sub> phase at position 34.51°. The zinc and manganese atoms in the Zn<sub>2</sub>Mn<sub>2</sub>Nb<sub>2</sub>O<sub>9</sub> compounds are ordered, and there is a decrease of symmetry (space group  $P3c1$ ) due to loss of the centres of inversion [23]. The XRD diffraction peak shift towards high angle and the interplanar spacing decreases with increase the Nd<sub>2</sub>O<sub>3</sub> concentration up to 0.04 mol% (Table 1). It occurs because the ionic radii of Nd<sup>3+</sup> (0.98 Å) are larger than Zn<sup>2+</sup> ions (0.74 Å). The disappearance of secondary phases at 0.05 mol% Nd<sub>2</sub>O<sub>3</sub> causes the peak shift towards low angle and increases the interplanar spacing. The similar results also reported by Aisah *et al.* [27] and Sri [28].

Table 1: Position  $2\theta$  (°) and  $d$ -spacing at various Nd<sub>2</sub>O<sub>3</sub> concentration.

Nd <sub>2</sub> O <sub>3</sub> (mol%)	Position $2\theta$ (°)	$d$ -spacing(Å)
0.01	34.39	2.4782
0.02	34.44	2.4750
0.03	34.48	2.4724
0.04	34.54	2.4684
0.05	34.39	2.4779

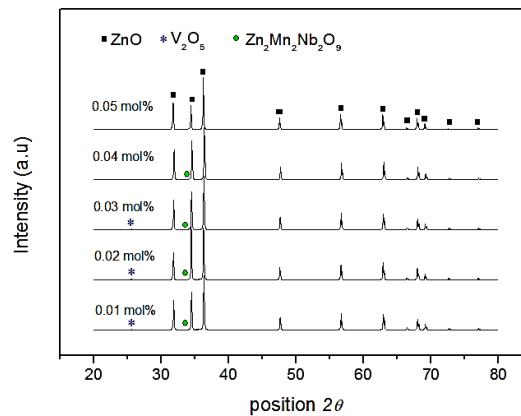


Fig. 1. XRD patterns at various  $\text{Nd}_2\text{O}_3$  concentration

The density ( $\rho$ ) of ZnO varistors ceramics was increased from 4.92 to 5.28  $\text{g}/\text{cm}^3$  with increasing  $\text{Nd}_2\text{O}_3$  concentration and its corresponding to 87.08 to 93.45% of the theoretical density. The  $\text{V}_2\text{O}_5$  liquid phase leading to densification of the sintered body and ZnO grain growth, since the eutectic temperature for  $\text{V}_2\text{O}_5$ -ZnO is about 600 °C. Instead of  $\text{V}_2\text{O}_5$  liquid phase, the densification was found to be enhanced by the addition of  $\text{Nd}_2\text{O}_3$  [29].

Fig. 2 shows the SEM micrographs of the samples with different  $\text{Nd}_2\text{O}_3$  concentration. The grain boundary is well separated and there is no exaggerated grain growth observed in all sample. The average grain size increased in the range from 3.36 to 3.54  $\mu\text{m}$  with the increase of  $\text{Nd}_2\text{O}_3$  concentration from 0.01 to 0.03 mol%. Further addition of it causes the value decreased to 2.54  $\mu\text{m}$  at 0.05 mol% attributed to the excessive  $\text{Nd}_2\text{O}_3$ . This indicates that the  $\text{Nd}_2\text{O}_3$  act as a grain enhancer at low concentration and as a grain inhibitor at high concentration, as agreed by Nahm et. al. [29] and Wang et. al. [30]. An intergranular pores are clearly seen in SEM image. At relatively low sintering temperature, the grain growth is not sufficient to produce a dense structure and could affecting the leakage current density value.

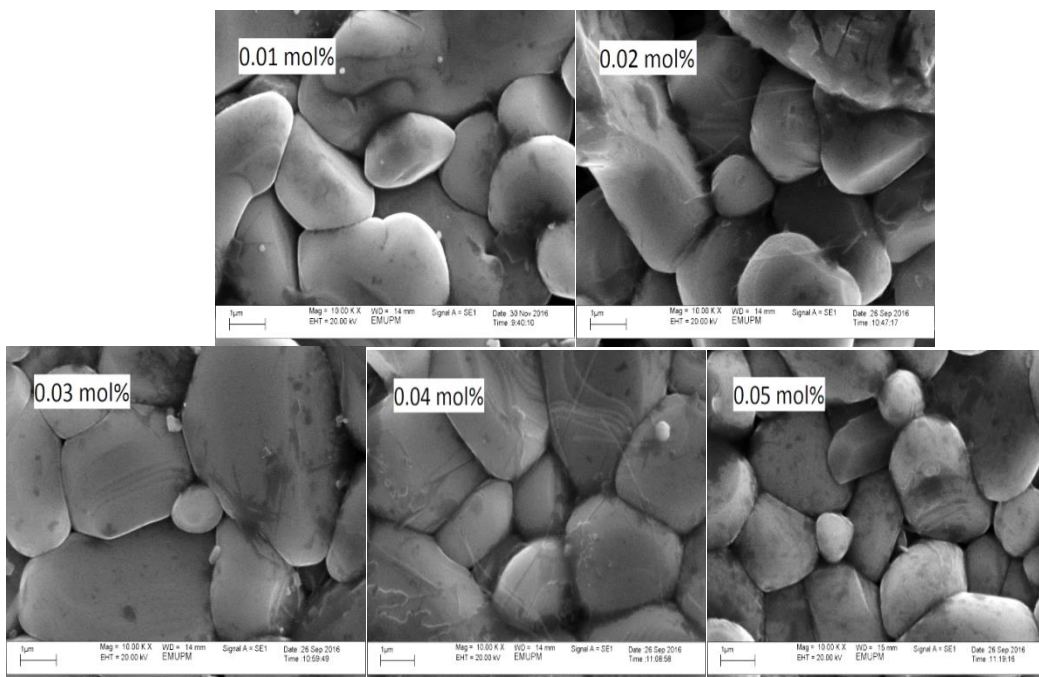


Fig. 2: SEM micrograph of sample at various  $\text{Nd}_2\text{O}_3$  concentration

Fig. 3 shows the  $J$ - $E$  curves of the samples where their properties are featured by the conduction characteristics which do not obey the ohm's law. Each curve exhibited two regions; (i) a linear region with high resistance before breakdown field and (ii) a nonlinear region with low resistance after breakdown field [11,12]. The sample modified with 0.03 mol% in the amount of  $\text{Nd}_2\text{O}_3$  exhibited more pronounced nonlinear properties in the vicinity of the knee. The  $J$ - $E$  parameters obtained from the characteristic curves are summarized in Table 2.

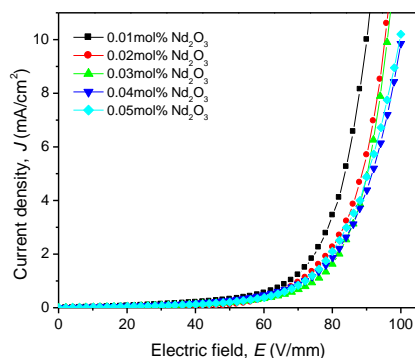


Fig. 3:  $J$ - $E$  curve at various  $\text{Nd}_2\text{O}_3$  concentration

Table 2: Average density ( $\rho$ ), relative density ( $\rho_{rel}$ ), grain size ( $D$ ), breakdown electric field ( $E_{1mA}$ ), nonlinear coefficient ( $\alpha$ ), leakage current ( $J_L$ ) and potential barrier height ( $\phi_B$ ) at various  $\text{Nd}_2\text{O}_3$  concentration

$\text{Nd}_2\text{O}_3$ (mol%)	$\rho$ (g/cm <sup>3</sup> )	$\rho_{rel}$ (%)	$D$ ( $\mu\text{m}$ )	$E_{1mA}$ (V/mm)	$\alpha$	$\phi_B$ (eV)	$J_L$ (mA/cm <sup>2</sup> )
0.01	4.92	87.08	3.36	68.00	8.72	0.561	0.39
0.02	4.95	87.61	3.45	72.07	8.86	0.627	0.27
0.03	5.02	88.84	3.54	75.05	9.94	0.679	0.22
0.04	5.10	90.27	3.30	72.03	7.26	0.532	0.39
0.05	5.28	93.45	2.54	70.07	7.10	0.529	0.41

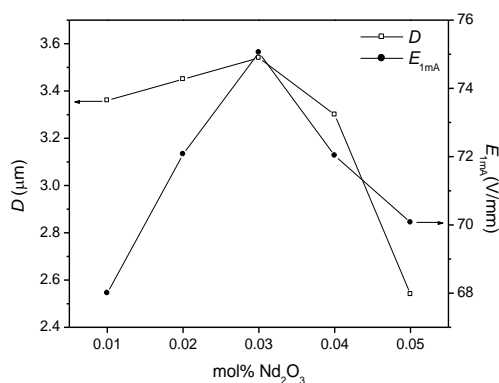


Fig. 4: The average grain size,  $D$  and breakdown field,  $E_{1mA}$  dependent on  $\text{Nd}_2\text{O}_3$  concentration

The  $E_{1mA}$  value was increased from 68.00 to 75.05 V/mm up to 0.03 mol%  $\text{Nd}_2\text{O}_3$  and further substitution disrupts the grain boundary characteristics when its value starts to drop to 70.07 V/mm at 0.05 mol%  $\text{Nd}_2\text{O}_3$ . The value of  $E_{1mA}$  varies in accordance with the  $\text{Nd}_2\text{O}_3$  content that can be explained by the following expression:

$$E_{1mA} = \frac{V_{gb}}{D} \quad (5)$$

where  $D$  is the grain size and  $V_{gb}$  is the breakdown voltage per grain boundaries. The high  $E_{1mA}$  value is attributed towards the decrease of average ZnO grain size and the increase of breakdown voltage per grain boundaries. However, the average grain size increase as the  $E_{1mA}$  value increases up to 0.03 mol%  $Nd_2O_3$ .  $Nd^{3+}$  ions act as acceptor ions, suppressed oxygen vacancy,  $V_O$  which make the resistance of the grains rise [31,32]. This two value decreases after this concentration. Besides, Nb-O bond length is shorter and its bond strength is stronger than Mn-O and Zn-O bond in the  $Zn_2Mn_2Nb_2O_9$  phase might increase the grains resistance [26].

The nonlinear  $\alpha$  has been used to estimate nonlinear properties quantitatively (Figure 5). The sharper knee of the curves leads to the good varistor properties. The behavior of  $\alpha$  can be related to the variation of the Schottky barrier height at the grain boundaries. The barrier height  $\phi_B$  increase from 0.561 to 0.679 eV and consequently increase the nonlinear  $\alpha$  value from 8.72 to 9.94 with increasing  $Nd_2O_3$  concentration up to 0.03 mol%. Due to the large ionic radii difference between  $Nd^{3+}$  ion which is 0.98 Å and  $Zn^{2+}$  ion which is 0.74 Å, the limited substitution of  $Nd^{3+}$  ion into Zn lattice generates additional zinc vacancy and oxygen since  $Nd_2O_3$  acts as an acceptor [33]. It has been well accepted that oxygen species promote the density of interface states, thus increasing the barrier height [33-37]. However, a further increase in  $Nd_2O_3$  concentration reduces the nonlinear  $\alpha$  value to about 7.10. The segregation of excessive rare earth oxide at the grain boundaries might have promoted the  $V_O$  formation and depleted the O species [37,38]. Thus, it reduces the density of interface state and decreases the barrier height.

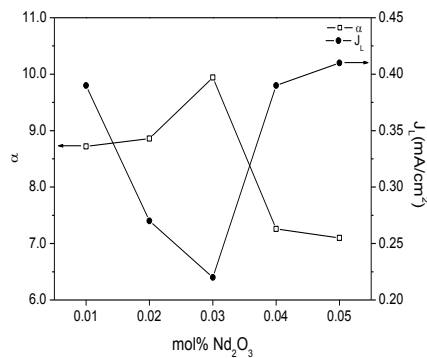


Fig. 5. The nonlinear coefficient,  $\alpha$  and leakage current density,  $J_L$  dependent on  $Nd_2O_3$  concentration

The value of  $\alpha$  and  $J_L$  depends on  $Nd_2O_3$  concentration as shown in Figure 5. The  $J_L$  behavior is always in contrast with  $\alpha$  value. The  $J_L$  value increases at the  $Nd_2O_3$  concentration above 0.03 mol% although sample density increases. The  $V_O$  formation increases the donor concentration since it is a deep donor which leads to a rise in  $J_L$  [31, 38]. As expected, it can be seen that sample modified with  $Nd_2O_3$  at low concentration has a significant effect on the nonlinear properties of these ceramics.

#### 4. Conclusions

In conclusion, a low-voltage varistor system based on Zn-V-Mn-Nb-O varistor ceramics with  $Nd_2O_3$  substitution has been presented. The effect of  $Nd_2O_3$  on the microstructure and electrical properties of Zn-V-Mn-Nb-O varistor ceramics sintered at 900 °C for 2 h has been investigated for the range of 0.01 to 0.05 mol%. The uniformity of the grain structure was improved with increasing the  $Nd_2O_3$  concentration. The limited substitution of  $Nd^{3+}$  ion inside the ZnO grain produces more oxygen that enhances the nonlinear  $\alpha$  value at a certain extent which is 0.03 mol% and decreases with excessive substitution as more oxygen is depleted at the grain

boundary and triple point junction.  $\text{Nd}_2\text{O}_3$  act as a grain enhancer at low concentration and as a grain inhibitor at high concentration.

### Acknowledgements

The authors are grateful to the Universiti Putra Malaysia for supporting this work under the Universiti Putra Malaysia GRANT No. GP-IPS/2016/9493000.

### References

- [1] T. K. Gupta, *J. Am. Ceram. Soc.* **73**(7), 1817 (1990).
- [2] L. M. Levinson, H. R. Philipp, *J. Am. Ceram. Soc. Bull.* **65**(4), 639 (1986).
- [3] K. Mukae *J. Am. Ceram. Soc. Bull.* **66**(9), 1329 (1987).
- [4] P. Cheng, S. Li, and M. A. Alim *Phys. Stat. Sol.* **204**(3), 887 (2007).
- [5] C. W. Nahm and B. C. Shin *Mater. Lett.* **57**(7), 1322 (2003).
- [6] C. W. Nahm *Trans. Nonferrous Met. Soc. Chi.* **25**(4), 1176 (2015).
- [7] H. H. Hng and L. Halim *Mater. Lett.* (8), 1411 (2003).
- [8] H. H. Hng and K. Y. Tse *Ceram. Intern.* **34**(5), 1153 (2008)
- [9] H. H. Hng and P. L. Chan *Ceram. Inter.* **30**(7), 1647 (2004)
- [10] H. H. Hng, K. M. Knowles, and P. A. Midgley *J. Am. Ceram. Soc.*, **84**(2), 435 (2001)
- [11] C. W. Nahm *J Mater Sci* **42**(19), 8370 (2007)
- [12] C. W. Nahm *Ceram. Inter.* **35**(2), 541 (2009)
- [13] C. W. Nahm *J Mater Sci: Mater Electron* **23**(9), 457 (2012)
- [14] S. Pandey, D. Kumar, and O. Parkash *Ceram. Inter.* **42** (8), 9686 (2016)
- [15] S. Bernik, M. Srećo, and B. Ai, *J. Europ. Ceram. Soc.* **21**(4), 1875 (2001).
- [16] D. Xu, X. F. Shi, X. N. Cheng, J. Yang, Y. Fan, H. M. Yuan, and L. Y. Shi *Trans. Nonferrous Met. Soc. Chi.* **20**(2), 2303(2010).
- [17] M. Houabes and R. Metz *Ceram. Inter.* **33**(7), 1191 (2007).
- [18] N. T. Hung, N. D. Quang, and S. Bernik *J. Mater. Res.* **16**(10), 2817 (2001).
- [19] W. R. W. Abdullah, A. Zakaria, M. Hashim, M. M. Rahman, and M. S. M. Ghazali *Mater. Sci. For.* **846**, 115 (2016).
- [20] C. W. Nahm *J. Am. Ceram. Soc.*, **94**(10), 3227 (2011).
- [21] C. W. Nahm *J Mater Sci: Mater Electron* **26**,10217 (2015)
- [22] C. W. Nahm *J Mater Sci: Mater Electron* **24** (12),4839 (2013).
- [23] J. C. Wurst and J. A. Nelson *J. Am. Ceram. Soc.* **55**, 109 (1972).
- [24] S. J. Dillon, S. K. Behera, M. P. Harmer, *Acta Mater.* **56**(6), 1374 (2008).
- [25] C. Li, J. Wang, W. Su, H. Chen, W. Wang, and D. Zhuang *Phys. Rev. B. Cond. Matter.* **307**(1), 1 (2001).
- [26] N. V. Tarakina, A. P. Tyutyunnik, V. G. Zubkov, T. V. Dyachkova, Y. G. Zainulin, H. Hannerz, and G. Svensson *Solid State Sciences* **5**(3), 459 (2003).
- [27] P. Sri *J. NanoSci. NanoTechnol.* **2** (1), 34 (2014).
- [28] N. Aisah , D. Gustiono , V. Fauzia , I. Sugihartono and R. Nuryadi. *IOP Conf. Series: Mater. Sci. Eng.* **172**, 1(2017).
- [29] C. W. Nahm, C. H. Park, and H. S. Yoon *J. of Mater. Sci. Lett.* **19**(4):271 (2000).
- [30] M. H. Wang, Q. H. Tang, and C. Yao *Ceram. Inter.* **36**(3), 1095 (2010).
- [31] A. Janotti and C. G. Van de Walle *Rep. Prog. Phys.* **72**(12), 126501(2009).
- [32] I. Gilbert and R. Freer *J. Phys.: Condens. Matter* **14**(4), 945 (2002).
- [33] L. Ke, M. Hu, and X. Ma *J. Mater.*, **2013**, 1(2013).
- [34] S. Bernik, S. Macek , B. Ai *J. of the Euro. Ceram. Soc.* **21**(10-11), 1875(2001).
- [35] E. R. Leite, J. A. Varela, E. Longo, *J. Mater. Sci*, **27**(19), 5325 (1992).
- [36] T. R. N. Kutty and S. Philip, *Mater. Sci. Eng. B*, **33**(2-3), 58 (1995).
- [37] W. R. W. Abdullah, A. Zakaria, and M. S. M. Ghazali *Int. J. Mol. Sci.* **13**(4), 5278 (2012).
- [38] C. W. Nahm, *J. Mater. Sci.* **41** (22), 7272(2006).